International Journal of Scientific Research in Science and Technology
Available online at : www.ijsrst.com
Print ISSN: 2395-6011 | Online ISSN: 2395-602X
doi : https://doi.org/10.32628/IJSRST52310632

The Feasibility of Cylindrical Step-Wedge Phantom for Evaluating Modulation Transfer Function of CT Image : Variation of Field of View

Neneng Kurnia Sari, Heri Sutanto, Choirul Anam, Ariij Naufal, Riska Amilia
Department of Physics, Faculty of Sciences and Mathematics, Diponegoro University, Jl. Prof. Soedarto SH, Tembalang, Semarang 50275, Central Java, Indonesia
Corresponding author: herisutanto@live.undip.ac.id

ARTICLEINFO

Article History:

Accepted: 10 Nov 2023
Published: 30 Nov 2023

Publication Issue
Volume 10, Issue 6
November-December-2023
Page Number
218-225

ABSTRACT

This study aims to evaluate the modulation transfer function (MTF) from a cylindrical step-wedge phantom having diameters of 8-32 cm at various field of views (FOVs). In this study, MTF curves were measured based on the edge spread function (ESF) using IndoQCT software. In addition, noises were also measured using IndoQCT software. It was found that the MTF curve decreased as the FOV increases. The difference in the MTF 10% from FOVs of 35-50 cm was 16-20% with a p-value of 0.392. Meanwhile, the difference in MTF 50% was 16-21% with the same p-value of 0.392. It was also found that MTF curve also decreased as the phantom diameter increases. The differences in MTF 10% and 50% from phantom diameter of 8-32 cm were 6-14% and 6-16%. It is resulted that the noise level decreases as the FOV increases and the noise level also decreased as the phantom diameter increases.

Keywords: Spatial resolution, modulation transfer function (MTF), edge spread function (ESF), field of view (FOV), cylindrical step-wedge water CT phantom

I. INTRODUCTION

Computed tomography (CT) scanner is a medical imaging modality that uses modern tomography and computerization techniques to examine human tissues or organs. The advancement of CT improves data acquisition process and image quality [1]. A high-quality image minimizes the misinterpretation of the resulting image, thus providing a more accurate diagnosis of a disease or disorder. Image quality is regularly monitored through a periodic quality control (QC) program. There are several parameter sets to determine image quality, including noise level, low contrast resolution, and spatial resolution [2].

Spatial resolution described the degree of sharpness of CT images. The spatial resolution of an imaging system can be characterized using the modulation

transfer function (MTF) curve. The curve represents the response of the imaging system for various spatial frequencies [3]. There are several methods in MTF measurement, including line spread function (LSF), point spread function (PSF), and edge spread function (ESF) [4]. The ESF method is more widely used because the edges are more accessible and does not require specific phantoms, such as wires or microbeads [5,6].

The spatial resolution of an image can be affected by several imaging parameters, such as focal spot size, slice thickness, reconstruction filter, and field of view (FOV) [7]. FOV is defined as the maximum diameter of the reconstructed image. Generally, the FOV value used in CT examinations is 12-50 cm [8]. Several studies had been conducted to evaluate spatial resolution using polymethyl methacrylate (PMMA) phantoms or built-in CT phantoms at various FOVs [9,10]. However, these studies were only applied to a single phantom diameter, whereas the size of the human body varies greatly. Therefore, it is important to investigate spatial resolutions at different phantom diameters, representing a wide range of human body sizes from paediatric to adult at FOV variation. This study aims to investigate the feasibility a cylindrical step-wedge phantom with a diameter of 8-32 cm for evaluating the spatial resolution with variation of FOV.

II. METHODS AND MATERIAL

A. Data acquisition of cylindrical step-wedge phantom

Spatial resolution measurements were performed using a cylindrical step-wedge phantom (Figure 1). The phantom was made of acrylic material with several diameters, including 8, 16, 24, and 32 cm. The phantom then filled with distilled water. This phantom was used to represent a wider range of human body sizes. Data acquisition of phantom images was performed using a GE Revolution EVO 128 slice CT scan at Indriati Solo Baru Hospital, Surakarta, Indonesia. The phantom was scanned using the parameter inputs shown in Table 1. The scanned images were saved in Digital Imaging and Communications in Medicine (DICOM) format. In this study, MTF measurements were performed using various FOVs variations (i.e., 35, 40, 45, and 50 cm). Axial phantom images of each diameter at various FOVs are shown in Figure 2.

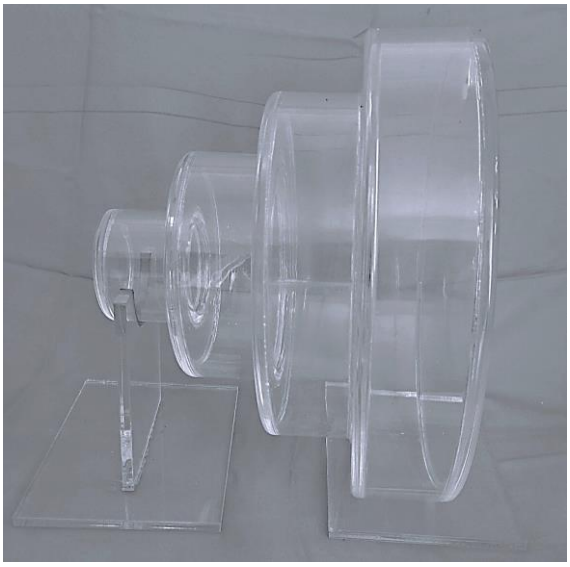

Figure 1. Photograph of cylindrical step-wedge phantom.

Table 1. Scan parameter for spatial resolution measurement.

Parameters	Input
Scan option	Helical
Tube voltage (kV)	120
Tube current (mA)	250
Reconstruction filter	Standard
Pitch	0.98
Slice thickness (mm)	5
Focal spot (mm)	1.2
FOV (cm)	35, 40, 45, and 50

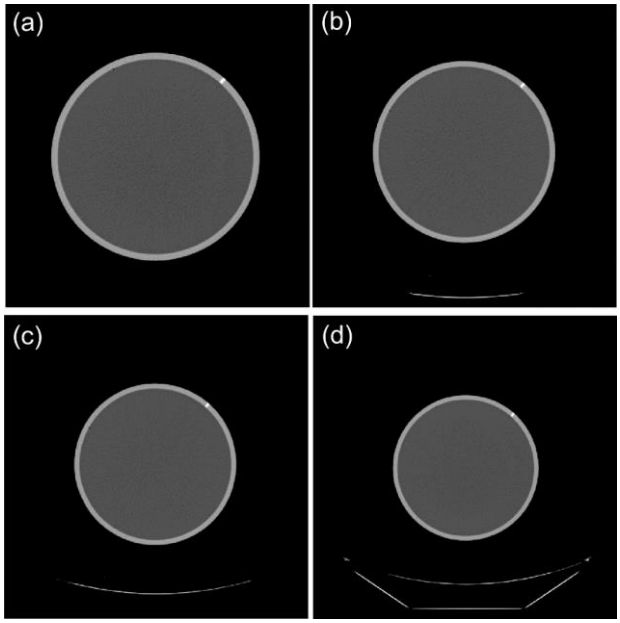

Figure 2. Axial images of phantom at phantom diameter of 24 cm for various FOVs: (a) 30 cm, (b) 40 cm, (c) 45 cm, and (d) 50 cm.

B. Automated measurement of spatial resolution

In this study, automatic spatial resolution measurement was performed using IndoQCT software [11]. The MTF curve was obtained from measurements using the edge spread function (ESF) method of the cylindrical step-wedge phantom. The region of interest (ROI) on the phantom edge was determined automatically. The profiles of the pixels were obtained within the ROI. The profile lines were then averaged to form a single ESF curve. The obtained ESF curve was then normalized to form the LSF curve. Next, a Fourier transformation was performed on the LSF curve to form the MTF curve. From the MTF curve, the spatial frequencies at MTF 50% and 10% were obtained. The spatial frequency at MTF 10% represents the spatial resolution limit corresponding to direct observation by the eye [12].

C. Noise measurement

In this study, noise from various of phantom diameters was measured. Noise measurement was performed using IndoQCT software. The noise was calculated from three slices of axial images of the phantom using a circle ROI in the center of the phantom (Figure 3). This noise measurement was performed to determine the difference in noise in the images generated from each phantom diameter and FOV used.

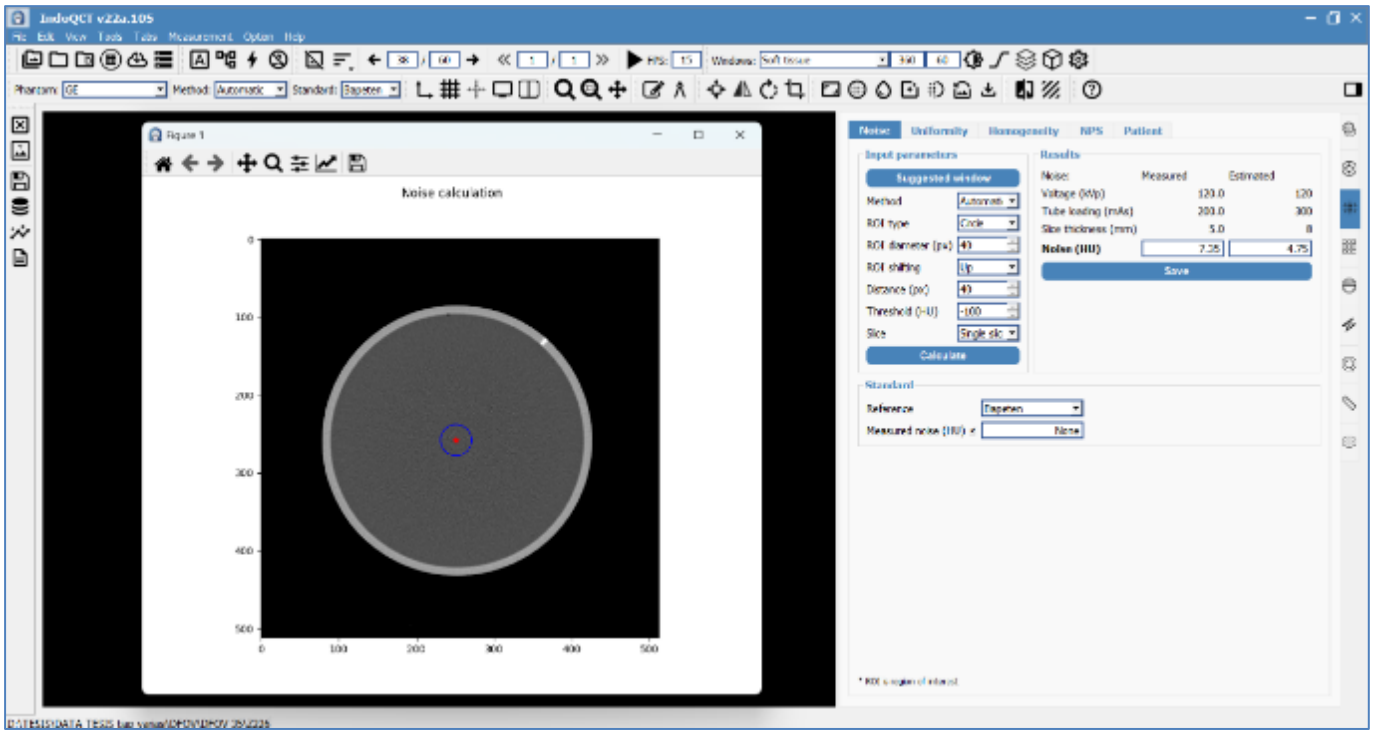

Figure 3. Graphical user interface (GUI) of IndoQCT software for noise measurement.

III.RESULTS AND DISCUSSION

A. Spatial Resolution of Cylindrical Step-wedge Water Phantom

MTF curves for FOV variation at diameters of 8-32 cm are shown in Figure 4. The MTF curve decreases as the FOV increases. An increasing FOV will result in an increase in pixel size in the image leading to decreasing MTF [12,13]. This phenomenon can be observed at all phantom diameter sizes. The difference in the MTF 10% from FOVs of 35-50 cm is 16-20% (Table 2) with a p-value of 0.392. Meanwhile, the difference in MTF 50% is 16-21% with the same p-value of 0.392. A p-value indicates that the difference in MTF value for FOV variation is not significant. Previously, Anam et al. [9] measured the MTF using a 16 cm diameter of PMMA phantom at FOVs of 20-35 cm and found that the MTF value increased with a decreasing FOV. Other studies have also reported that a narrow FOV can improve the spatial resolution of the image [14-16]. The consistency of the results obtained in the current with previous studies indicates the applicability of the cylindrical step wedge phantom as a tool in evaluating spatial resolution.

MTF curves for various diameters at different FOVs are shown in Figure 5. It shows that the resulting MTF curve decreases with increasing phantom diameter. The difference in MTF 10% from phantom diameter of 8-32 cm is 6-14% (Figure 2). At the same time, the difference in MTF 50% is 6-16%. The decrease in MTF value at a larger phantom diameter occurs due to the difference in the projected focal spot between the edge of the phantom located at different positions from the iso-center [17]. The larger diameter of the phantom leads to the greater distance from iso-center, which leads to decrease spatial resolution [18,12]. Based on the results, FOV is more influencing spatial resolution compared to phantom diameter. However, the influence of the phantom diameter cannot be ignored to obtain a more accurate spatial resolution value.

Table 2. Results of spatial resolution measurements for various phantom diameter with different FOVs.

Phantom diameter (cm)	Spatial frequency (cycles/mm)							
	FOV 35 cm		FOV 40 cm		FOV 45 cm		FOV 50 cm	
	MTF 10%	MTF 50%	MTF 10%	MTF 50%	MTF 10%	MTF 50%	MTF 10%	MTF 50%
8	0.65	0.38	0.57	0.33	0.54	0.32	0.52	0.30
16	0.61	0.35	0.57	0.34	0.52	0.31	0.50	0.30
24	0.58	0.33	0.56	0.32	0.52	0.30	0.47	0.28
32	0.56	0.32	0.54	0.31	0.51	0.29	0.47	0.27

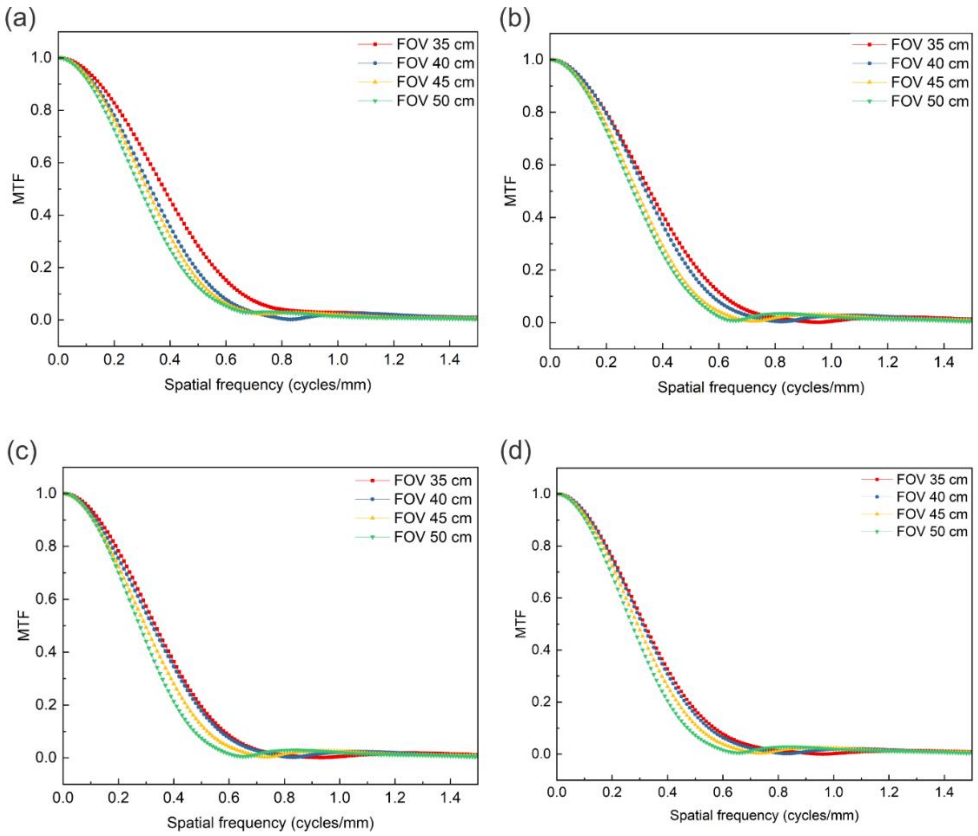

Figure 4. The comparisons of MTF curves with various FOVs for different phantom diameters: (a) 8 cm, (b) 16 cm, (c) 24 cm, and (d) 32 cm.

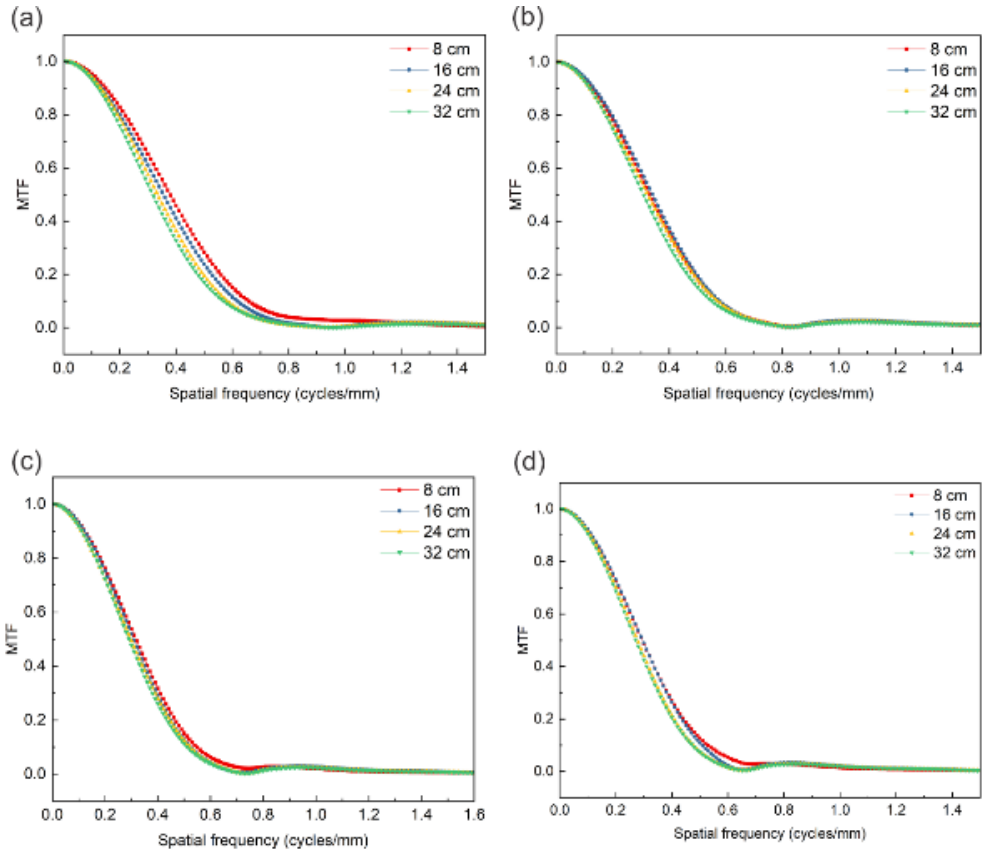

Figure 5. The comparisons of MTF curves with various diameters for different FOVs: (a) 35 cm, (b) 40 cm, (c) 45, and (d) 50 cm.

B. Noise of Cylindrical Step-wedge Water Phantom

Noise levels of FOV variation at diameter of 8-32 cm are shown in Figure 6. It shows that the noise decreases as the FOV increases. At phantom diameter of 8 cm, the highest noise is generated at an FOV of 35 cm, which is 1.62 HU. While the lowest noise is generated at a FOV of 50 cm, which is 1.2 HU. High noise in the image causes fluctuation in the resulting MTF curve [9]. This will affect the accuracy of the measurements.

Noise levels for various phantom diameters at different FOVs are shown in Figure 7. It clearly shows that the noise increases as the phantom diameter increases. At FOV 35 cm, a phantom diameter of 8 cm produces the lowest noise of 1.62 HU. Meanwhile, the 32 cm diameter phantom has the highest noise of 16.08 HU. According to the Beer-Lambert Law (BLL), the thickness of an object greatly affects the intensity of absorbed X-ray radiation [20-22]. Therefore, the transmitted photons through phantom having large diameter will decrease and it leads to decrease image noise.

This study has several limitations. First, the developed in-house phantom is still under development, hence it is necessary to compare the result with a standard phantom before being applied in a QA setting. Another limitation is that the measurement of spatial resolution using the cylindrical step-wedge phantom is only performed on a single CT scanner. Therefore, measuring spatial resolution from other CT scanners for proving dependence of MTF with phantom diameter.

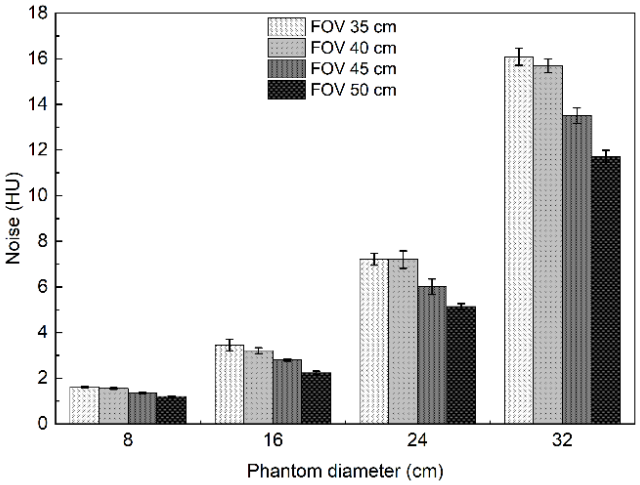

Figure 6. Comparison of noise levels with various FOVs for different phantom diameters.

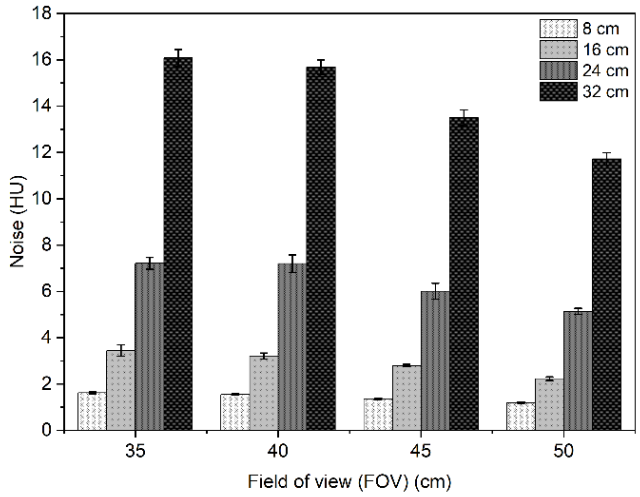

Figure 7. Comparison of noise levels with various phantom diameters for different FOVs.

IV. CONCLUSION

In conclusion, the spatial resolution decreased with increasing FOV. Meanwhile, the spatial resolution also decreased with the phantom diameter. The MTF 10% difference from 8-32 cm phantom diameter at the FOV variation is 5.26-13.84%. While the MTF 50% difference is 6-15.8%.

V. ACKNOWLEDGEMENTS

This work was funded by Riset Publikasi Internasional Bereputasi Tinggi (RPIBT), Diponegoro University, with contract number 609-120/UN7.D2/PP/VIII/2023.

VI. REFERENCES

[1] Bankier AA, Kressel HY. Through the Looking Glass revisited: the need for more meaning and less drama in the reporting of dose and dose reduction in CT. *Radiology*. 2012;265(1):4-8. doi:10.1148/radiol.12121145

[2] Nakahara S, Tachibana M, Watanabe Y. One-year analysis of Elekta CBCT image quality using NPS and MTF. J Appl Clin Med Phys. 2016 May 8;17(3):211-222. doi: 10.1120/jacmp.v17i3.6047. PMID: 27167279; PMCID: PMC5690923.

[3] Xie X, Fan H, Wang A, Zou N, Zhang Y. Regularized slanted-edge method for measuring the modulation transfer function of imaging systems. *Appl Opt*. 2018;57(22):6552-6558. doi:10.1364/AO.57.006552

[4] Maruyama S. Assessment of Uncertainty Depending on Various Conditions in Modulation Transfer Function Calculation Using the Edge Method. *J Med Phys*. 2021;46(3):221-227. doi:10.4103/jmp.JMP_36_21

[5] Kayugawa A, Ohkubo M, Wada S. Accurate determination of CT point-spread-function with high precision. *J Appl Clin Med Phys*. 2013;14(4):3905. Published 2013 Jul 8. doi:10.1120/jacmp.v14i4.3905

[6] Manson EN, Bambara L, Nyaaba RA, et al. Comparison of Modulation Transfer Function Measurements for Assessing The Performance of Imaging Systems. Medical Physics. 2017;5(2):188-191.

[7] Kim, K. B., Jeong, S. H., Lee, S. H., & Kim, K. (2021). Investigation of patch-based modulation transfer function (MTF) prediction framework in radiography. *Radiation Physics and Chemistry*, *189*. https://doi.org/10.1016/j.radphyschem.2021.109728

[8] Valzano, S., & Matheoud, R. (2014). Quality Controls in x-Ray Imaging. In *Comprehensive Biomedical Physics* (pp. 167–191). Elsevier. https://doi.org/10.1016/b978-0-444-53632-7.00208-2

[9] Anam C, Fujibuchi T, Budi WS, Haryanto F, Dougherty G. An algorithm for automated modulation transfer function measurement using an edge of a PMMA phantom: Impact of field of view on spatial resolution of CT images. *J Appl Clin Med Phys*. 2018;19(6):244-252. doi:10.1002/acm2.12476

[10] Nofrianto, Choirul Anam, Eko Hidayanto, Ariij Naufal. Comparison of MTFs Measured using IndoQCT and ImQuest Software on GE CT Phantom Images. Int J Sci Res Sci Technol [Internet]. 2023 Jun 16;852–8. Available from: https://ijsrst.com/IJSRST523103156

[11] Anam C, Naufal A, Budi WA, Sutanto H, Haryanto F, Dougherty G. (2023). Manual IndoQCT Version 22a. Undip Press

[12] Zhang J, Bao Z, Huang X, Jiang D, Xie C, Zhou Y. Methods to evaluate the performance of kilovoltage cone-beam computed tomography in the three-dimensional reconstruction space. Int J Radiat Res. 2019; 17(2) :189-202. doi: http://ijrr.com/article-1-2494-en.html

[13] Salimova N, Hinrichs JB, Gutberlet M, Meyer BC, Wacker FK, von Falck C. The impact of the field of view (FOV) on image quality in MDCT angiography of the lower extremities. *Eur Radiol*. 2022;32(5):2875-2882. doi:10.1007/s00330-021-08391-x

[14] Safi Y, Ghazizadeh Ahsaie M, Jafarian Amiri M. Effect of the Field of View Size on CBCT Artifacts Caused by the Presence of Metal Objects in the Exomass. *Int J Dent*.

2022;2022:2071108. Published 2022 Sep 9. doi:10.1155/2022/2071108

[15] Miyata T, Yanagawa M, Hata A, Honda, O, Yoshida Y, Kikuchi N, Tsubamoto M, Tsukagoshi S, Uranishi A, Tomiyama N. Influence of field of view size on image quality: ultra-high-resolution CT vs. conventional high-resolution CT. *Eur Radiol*. 2020;30(6):3324-3333. doi:10.1007/s00330-020-06704-0

[16] Niktash A, Mehralizadeh S, Talaeipour A. The Effect of Different Field of View Sizes on Contrast-to-Noise Ratio of Cone-Beam Computed Tomography Units: An In-Vitro Study. *Front Dent*. 2022;19:32. Published 2022 Sep 18. doi:10.18502/fid.v19i32.10804

[17] Takenaga T, Katsuragawa S, Goto M, Hatemura M, Uchiyama Y, Shiraishi J. Modulation transfer function measurement of CT images by use of a circular edge method with a logistic curve-fitting technique. *Radiol Phys Technol*. 2015;8(1):53-59. doi:10.1007/s12194-014-0286-x

[18] Cho HW, Yoon HJ, Yoon JC. Analysis of crack image recognition characteristics in concrete structures depending on the illumination and image acquisition distance through outdoor experiments. *Sensors (Basel)*. 2016;16(10):1646. doi:10.3390/s16101646

[19] Zarb, F., Rainford, L., & McEntee, M. F. (2010). Image quality assessment tools for optimization of CT images. In *Radiography* (Vol. 16, Issue 2, pp. 147–153). https://doi.org/10.1016/j.radi.2009.10.002

[20] Solomon J, Wilson J, Samei E. Characteristic image quality of a third generation dual-source MDCT scanner: Noise, resolution, and detectability. *Med Phys*. 2015;42(8):4941-4953. doi:10.1118/1.4923172

[21] Oshina I, Spigulis J. Beer-Lambert law for optical tissue diagnostics: current state of the art and the main limitations. *J Biomed Opt*. 2021;26(10):100901. doi:10.1117/1.JBO.26.10.100901

[22] Mayerhöfer TG, Pahlow S, Popp J. The Bouguer-Beer-Lambert Law: Shining Light on the Obscure. *Chemphyschem*. 2020;21(18):2029-2046. doi:10.1002/cphc.202000464

Cite this article as :

Neneng Kurnia Sari, Heri Sutanto, Choirul Anam, Ariij Naufal, Riska Amilia, "The Feasibility of Cylindrical Step-Wedge Phantom for Evaluating Modulation Transfer Function of CT Image : Variation of Field of View", International Journal of Scientific Research in Science and Technology (IJSRST), Online ISSN : 2395-602X, Print ISSN : 2395-6011, Volume 10 Issue 6, pp. 218-225, November-December 2023. Available at doi : https://doi.org/10.32628/IJSRST52310632
Journal URL : https://ijsrst.com/IJSRST52310632